# Computational Insight into the Interaction of Cytochrome c with Wet and PVP-Coated Ag Surfaces

Francesco Tavanti[a], Alfonso Pedone[a], Paolo Matteini[b] and Maria Cristina Menziani[a*]

[a] Department of Chemical and Geological Sciences, University of Modena and Reggio Emilia, Via G. Campi 103, 41125 Modena, Italy.
[b] Institute of Applied Physics "Nello Carrara", National Research Council, Via Madonna del Piano 10, 50019 Sesto Fiorentino, Italy.

***Corresponding Author**

Prof. Maria Cristina Menziani, PhD
University of Modena and Reggio Emilia
Department of Scienze Chimiche e Geologiche
Via Campi 103
41125 Modena -Italy
Tel: +39-059-2058555
E-mail: mariacristina.menziani@unimore.it

**Abstract**

In this work, the adsorption of Cytochrome C (CytC) on wet {100}, {111}, {110} and {120} silver surfaces has been investigated by computational simulations. The effect of Polyvinylpyrrolidone (PVP) coating has also been studied. The main results obtained can be summarized as follow: a) CytC strongly interacts with wet bare high index facets, while the adsorption over the {100} surface is disfavoured due to the strong water structuring at the surface; b) a non-selective protein adsorption mechanism is highlighted; c) the native structure of CytC is well preserved during adsorption; d) the heme group of CytC is never found to interact directly with the surface; e) the interactions with the PVP-capped {100} surface is weak and specific. These results can be exploit to better control biological responses at engineered nano-surface, allowing the development of improved diagnostic tools.

## Introduction

Understanding the mechanism of interaction between proteins and metal surfaces of nanostructured materials is a crucial task to advance the design of new safer and more efficient therapeutic, diagnostic, and sensing tools[1,2].

Despite substantial progress, characterization of the absorption process at the molecular level by experimental means is still very challenging and limited to a few properties[3–5] Moreover, the complex interplay among the physico-chemical properties of the metal surface (size, morphology, charge, coating), of the protein(s) (sequence, structure, and dynamics, concentration) and of the environmental conditions (surfactants, solvent, ionic strength, and pH) often leads to unclear contradictory evidences, making the interpretation of the results difficult.

Computational approaches have the potential to provide molecular insight not directly accessible by experimental studies, and can effectively complement experiments to design well-defined nanosurfaces able to modulate and control biological responses. Recent studies on protein adsorption on metal surfaces and overviews of their possible applications are reported in refs[6–8] and references therein.

Many computer simulation studies have focused on the interactions of biomolecules onto the commonly featured {111} and/or {100} bare Au, Ag, Cu, Fe, Pd, Pt surfaces[6,7], (see refs 6 and 7 for comprehensive recent reviews) whereas only a few studies have addressed functionalized metal surfaces[7,9,10]. Moreover, little attention has been paid in the literature to the influence of the topography of nanocrystal surfaces on their binding characteristics toward biomolecules[11,12], although it has been recognized as critical in order to obtain realistic model useful for real-life applications[6].

Recently, some of us were involved in a combined experimental and computational study aimed at verifying the opportunity to obtain efficient biodiagnostic tools by exploiting the selectivity of different crystal planes of silver nanocubes for the Polyvinylpyrrolidone (PVP) polymers and Cytochrome C (CytC)[13].

Briefly, we found that the PVP capping agent, besides assuring an elevated colloidal stability, shows a preference for the cube side faces {100}[14], conferring regional passivation and driving the preferential interaction of the protein with the corners, which surfaces are composed of a mixture of high Miller index facets, preferentially {110} and {120}. Thus, this system appears an ideal surface-enhanced Raman (SER) substrate for protein detection since the intensified electromagnetic fields experienced by the protein on the corners provide efficiency and detection sensitivity while undesirable signal fluctuations caused by molecular adsorption to different areas of the nanocrystal surface are circumvented. Thus, this system is an

ideal SER substrate since the intense electric field experienced by the proteins enhances efficiency and detection sensitivity. Moreover, undesirable signal fluctuations caused by molecular adsorption to different zones of the nanocrystal are circumvented. In this study, CytC, a hemoprotein part of the electron transport chain of mitochondrial respiration, was used as it is a low abundance biomarker of principal biological processes, such as the incurrence of malignant tumours and fulminant hepatitis, and represents a model protein well characterized in Raman and resonant-SER spectroscopy (SERS) studies[15].

Our preliminary computational results obtained in this study[13] highlight the necessity of a deeper understanding of the forces governing the selectivity of proteins towards silver surface planes. In fact, in contrast to the extensive computational investigations on the interactions of protein with Au surfaces, the Ag surfaces have been often disregarded, although differences in the biomolecule binding to the two metal surfaces have been recognized[16]. Moreover, the computational studies on Ag present in the literature up to now focus on the most common {111}[16–18]and {100}[18] surfaces only, and involve interaction with small peptides[16–19]. The relative simplicity of small peptide assures that their absorption free energy can be computed with high accuracy using advanced sampling approaches. However, the results can not be directly extended to proteins whose binding characteristics to the metal surface are dictated by a well-defined tertiary structure.

Here, we present a molecular dynamics simulation study that systematically investigates, for the first time in the literature, the binding modalities of CytC to wet silver surfaces with four different facet indexes ({100}, {111}, {110} and {120}). The role of PVP coating in the protein-metal surface interactions is also analysed. The mechanistic features of protein adsorption to Ag surfaces revealed here can be extended to other facets, proteins and coatings. Therefore, the results obtained can be instrumental for the design of optimal protein–surface interactions to be used as early diagnostic tools.

## Methods

### Computational details

The structure of the bovine heart CytC[20] was retrieved from the RCSB data bank[21] (PDB ID: 2B4Z). The CHARMM27[10,22] force field (FF) was used for the protein, whereas the parameters for the heme prosthetic group were obtained from Autenrieth et al.[23] Standard protonation states corresponding to pH 7 were assigned to ionizable residues.

The {100} and {111} Ag surfaces were simulated using two FFs: the AgP-CHARMM FF developed by Hughes et al.[18] and the FF from Heinz et al.[24], which is compatible with the CHARMM FF, as previously demonstrated by Penna et al.[25]. The AgP-CHARMM FF developed by Hughes et al.[18] takes into account the electric metal polarization by employing virtual interaction sites on the Ag surface and capturing polarization via the rigid-rod dipole approach[26]. The FF from Heinz et al.[24], on the contrary, furnishes improved Lennard-Jones parameters for the simulation of several face-centred cubic metals and hybrid interfaces. The results are typically an order of magnitude more accurate than previous LJ parameters due to the physical interpretation of the parameters in terms of the metal density and the surface tension of the {111} crystal face under standard conditions.

The Ag surfaces models, obtained according to the two FFs and used as input in the molecular simulations studies, are shown in **Figure 1**, where the Ag {100} is reported, as an example.

In the model of flat surface consistent with the AgP-CHARMM FF developed by Hughes et al.[18] five slabs of Ag atoms are built according to the symmetry of the surface chosen. Atoms in the outer layers are called Ag Surface (AGS), while atoms in the inner layers are called Ag Bulk (AGB) (**Figure 1a**). As in the GoldP-FF[26], atoms representing the virtual interaction sites, Ag Interaction (AGI), are added to the outer layers to drive absorption on the preferential surface sites. Their spatial positions follow the same pattern as the AGS atoms, but are shifted to occupy the hollow sites (see **Figure 1b**). These atoms are neutrally charged, and they interact with adsorbing species via the Lennrad-Jones terms. Finally, atoms called Ag Charged (AGC) with a mass of 0.5u are added to AGB and AGS atoms at the distance of 0.07nm (**Figure 1c**). In order to reproduce the electronic metal polarization a net charge of 0.308e is assigned to the AGC atoms, whereas a charge of -0.308e is assigned to the AGB and AGS atoms obtaining a neutral polarized system ("rigid-rod" dipoles[27]), see **Figure 1 c, d**. The rigid-rod dipole particles were free to rotate during MD simulations according to their thermostat temperature, whereas the other silver atoms were held fixed in the space.

In the model of flat surface consistent with the Heinz et al.[24] FF only one kind of atom (that we called AG) is considered. These AG atoms are held fixed in their positions during simulations and are characterized by accurate Lennard Jones potential; no charges are assigned (**Figure 1e**).

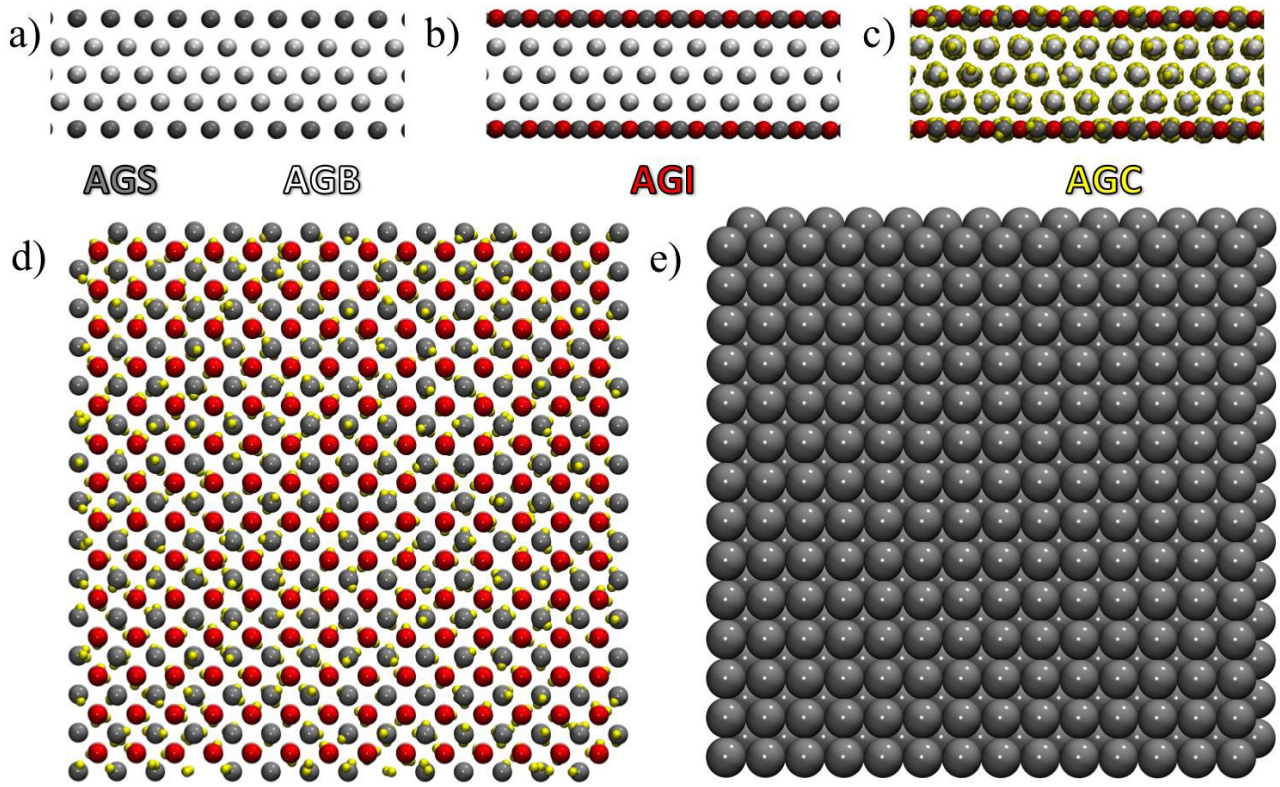


**Figure 1:** The {100} Ag surface models: in panels a), b) and c) lateral, and d) top views of the Ag surface model according to Hughes et al.[18] Atoms are coloured according to their names: AGS in silver, AGB in white, AGI in red and AGC in yellow. In panel e) the Ag surface according to the Heinz et al.[24] model.

On the basis of the similarity of the results obtained for the {100} and {111} Ag surfaces with the two FF, only the FF from Heinz et al.[24] was used for the {110} and {120} surfaces.

Four CytC proteins were inserted in a simulation box in random positions, with random orientations. A minimum distance of 2 nm from the Ag surfaces located at the bottom of the simulation box and of 1 nm among the protein surfaces were assured in order to avoid any possible initial bias of the proteins facing the surfaces and of the protein-protein interactions (see **Figure 2a**).

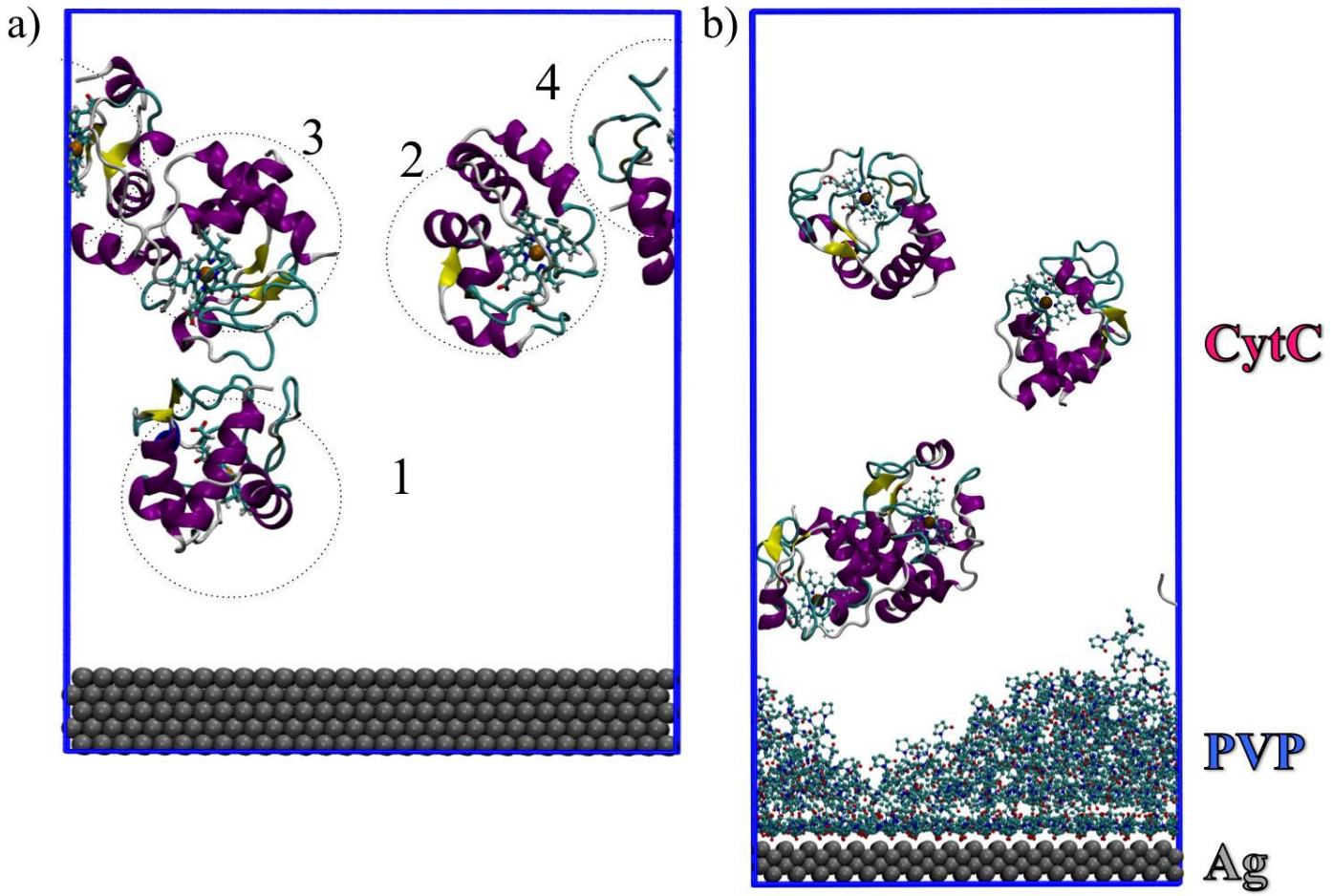


**Figure 2**: Representative examples of the initial configurations used in the molecular simulations. Four CytC proteins randomly placed in the simulation boxes with the Ag surface (panel a) and with the PVP-coated Ag surface (panel b) at the bottom (water and ions are not shown for clarity).

The final dimension of the simulation box for the system containing the {100} surface was 8.82x8.82x8.00nm (the dimensions of the other simulation boxes are listed in **Table S.1** in SI). Periodic boundary conditions were applied.

In order to avoid interactions of proteins with the periodic image of the Ag surface, a layer of dummy atoms carrying repulsive Lennard-Jones potential with $\sigma$=0.3nm and $\varepsilon$=0 kJ/mol was placed on the top of the box. In this way, by running each computational twice for each surface (with different initial random positions and velocities assigned to the four CytC proteins in the simulation box) eight CytC independent replicas were obtained. The systems were solvated using the modified TIP3P water model (TIPS3P)[18], which is compatible

with both Ag FFs[25]. Ions and counter-ions ($Na^+$ and $Cl^-$) were added in the minimal amount to reach charge neutrality with a physiological concentration of 150mM.

To simulate a PVP (Polyvinylpyrrolidone)-covered {100} Ag surfaces, chains of PVP containing 22 monomers were built using the force field from Kyrychenko et al.[28]. Then 27 PVP polymers were inserted in a rectangular box (8.82x8.82x11.0nm) with the Ag {100} surface at the bottom and a NVT simulation without water was conducted until all polymers were adsorbed on the metal surface. In the final configuration 2 layers of PVP were adsorbed on the surface (called inner and outer, in the following) in agreement with experimental results[13]. Then four Cytochrome C proteins, water and ions were added using the same procedure as for the other simulations, see **Figure 2b**.

The long-range electrostatics were computed using the particle-mesh Ewald (PME) algorithm[29,30] a fourth-order cubic interpolation, a grid spacing of 0.16nm, and a real-space cutoff of 1.3nm[18,31]. Both Van Der Waals and neighbour list cutoffs describing short-range interactions were set to 1.0 nm. The temperature in all simulations was kept constant at the physiological value of 310K and the pressure was set to 1 bar in order to mimic physiological conditions. Maxwellian distribution at the given temperature was used to assign random velocities to atoms.

The systems were minimized and thermalized using the following procedure. First, an energy minimization was performed using the steepest descent algorithm for 5000 steps. Then, the system was equilibrated using the NVT ensemble for 2ns, with the temperature controlled by means of a velocity-rescaling thermostat with a coupling time of 0.1ps. All bonds were constrained by using the LINCS algorithm[32]. During equilibration, positions restraints to heavy atoms of protein were applied, allowing the water to thermalization and equilibration only. Then, all the restraints were removed and a 10ns NPT equilibration run was performed by controlling the pressure with the Berendsen barostat. Finally, 100ns long production runs with the timestep set to 2.0fs were performed. In this step, the pressure was controlled by means of the Parrinello-Rhaman barostat with coupling time of 2ps and an isothermal compressibility of $4.5 \times 10^{-5}$ $bar^{-1}$. Two replicas with different CytC starting positions and velocity distributions were considered.

Computational simulation were performed using the Gromacs_5.0.4 package[33] and trajectory visualization and molecular rendering were carried out with VMD_1.9.2[34].

Binding energies were computed by means of the Molecular Mechanics Poisson-Boltzman Surface Area (MM-PBSA) method. A short description of this method can be find in the SI. The calculation of the binding energies was performed over 2000 frames, i.e. 20ns, in the region of the simulations where the CytC is stably bound to

the surface. If the protein was found to bind to the surface only after 80 ns of the total simulation time (100 ns), the simulation was extended to ensure the sampling of 2000 frames.

The orientation of the HEME dipole angle with respect to the normal of the surface was monitored (**Figure S.1** in SI), and visual inspection of the trajectories was carried out to check that a stable binding of the CytCs to the Ag surfaces[13] was reached.

## Results and Discussion

### The Ag wet surfaces

**Figure 3** shows the structural organization of the water molecules on the four Ag surfaces studied, as detected by the 2-dimensional density profiles computed along z-direction (perpendicular to the surface).

Water in proximity of the surfaces is strongly structured and forms a first layer of molecules at around 3.5 Å, and a second one at around 5.0 Å from the Ag surface. Overall, this phenomenon is shared by all the surfaces studied, and seems to be independent from the FF used to model the Ag surfaces (see **Figures 3a** and **3b** for the {100} and {111} surfaces, respectively. Moreover, overall the ordering of water at the {100} facets is greater with respect to the other surfaces, as already pointed out by recent studies on water organization at metal surfaces[17,18,31,35]

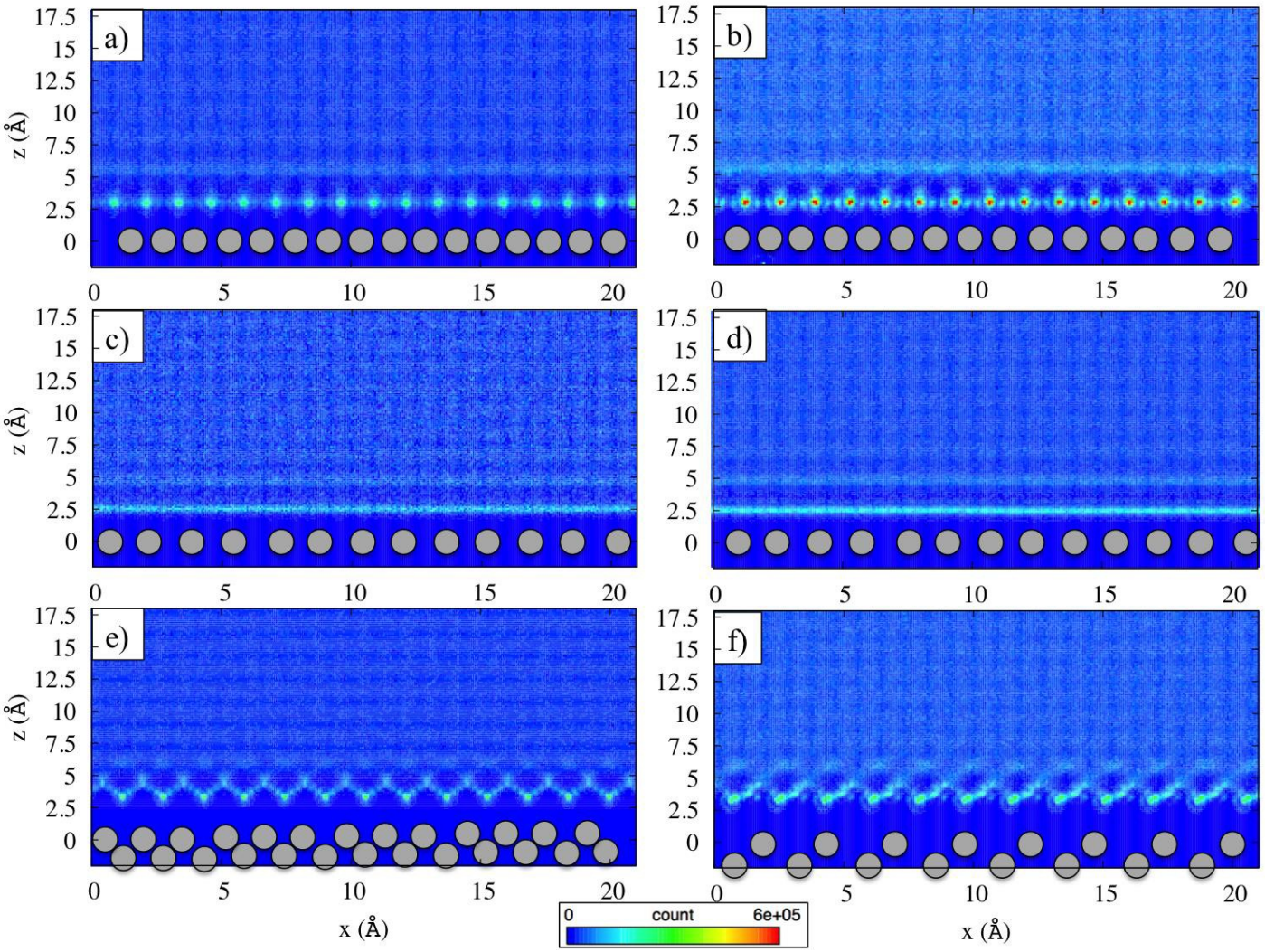


**Figure 3:** 2-dimensional density profiles of water oxygen atoms at different silver surfaces computed along z-direction (perpendicular to the surface): a) and b) for the {100} using the AgP-CHARMM FF[18]and the FF from Heinz et al.[24], respectively; c) and d) for the {111} using the AgP-CHARMM FF[18]and the FF from Heinz et al.[24], respectively; e) for the {110} and f) for the {120}. Grey spheres represent silver atoms. On the bottom, the color-scale used.

**Cytochrome C binding modalities**

The analysis of the minimum distance between a given amino acid residue and the Ag surfaces during the simulation time is useful to gain a first glance on the adsorption modalities of CytC. **Figure 4** shows the minimum distance evolution during the dynamic runs for four exemplary computational simulations.

As previously proposed for the adsorption of proteins and peptides on gold nanoparticles and flat surfaces[25,36–40], protein adsorption on Ag takes place in three steps. At the beginning of the simulation, the four proteins are free to move in the box and the approach to the surface is controlled by diffusion. Occasional protein-protein encountering with a life-time of the complex of less than 5% of the total simulation time is observed. During this period, large fluctuations of the minimum protein-surface distance data values are observed. In the second step CytC residues start to interact with the layers of structured water molecules, break through them occasionally, and achieve temporary docking to the Ag surfaces. It is interesting to note that this reversible process lasts for different simulation times for the different facets (i.e. on average 15, 20 , 25 and 30 ns, standard deviation around 30%, for the {110}, {111}, {100} and {120} facets, respectively). Visual inspection of the trajectories reveals peculiarities in the behaviour of the proteins during this step. Proteins on the {100} facets remain entrapped in the double layer of water molecules on the surface (see **Figure S.2**) before being able to break through and adjust on the metal surface to realize stable binding (third step). Whereas permeation of amino acid residues of CytC through the water layer adjacent to the {110} facet is easier and stable interactions are realized since the early nanoseconds of the total simulations time. In the case of Cyt on the {111} facet sporadic interactions of the incoming protein with an already bound protein complicate the adsorption process. Finally, in the case of the {120} surface several docking events are required before reaching stable interactions. As shown in the following paragraphs, this may be ascribed to the hydrophobic nature of the amino acid residue, which constitute the binding sites for the {120} surface.

Therefore, differences in the binding characteristics of CytC with respect to the various Ag facets originate from an interplay of several phenomena. However, the ability of the protein to displace the water molecules from the first structured layer over the Ag surfaces of different indexes plays an important role in all the models studied. Similar results on the role of the water layer in the adsorption of small peptides onto metal surfaces have been reported recently in the literature[16,25,41].

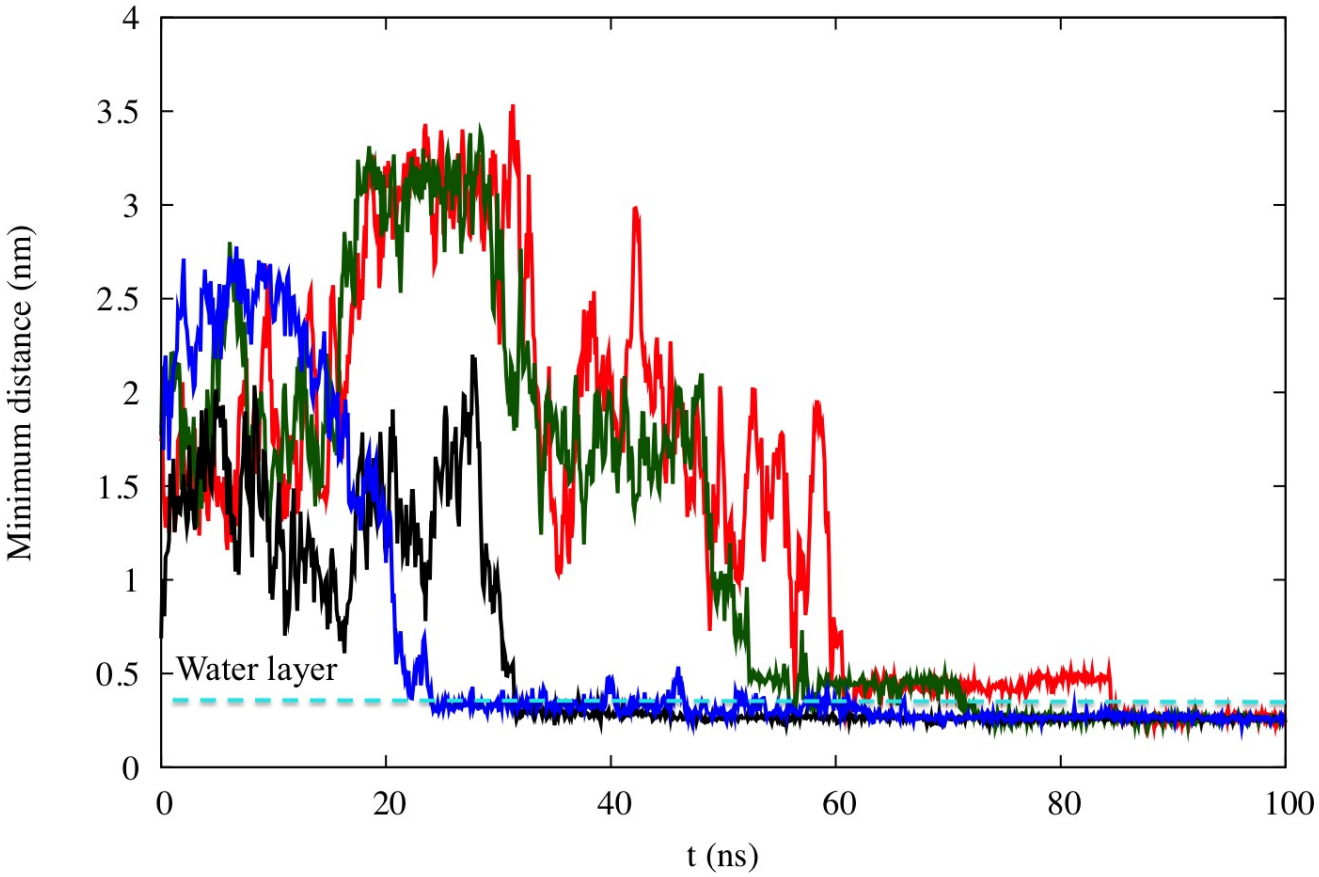


**Figure 4:** The minimum distance between CytC and the Ag surfaces during the 100 ns production run. The cyan dashed line placed at 3.5Å from the Ag surface represents the polarized water layer. Data show one representative simulation for each Ag facet (red: {100}; green: {111}; black: {110} and blue: {120}).

The binding modalities of CytC on Ag surfaces have been analysed further by tracking the protein regions that contact the metal surface and produce persistent interactions during the course of the computational simulations. In this context, a contact is established when the distance between an atom of the protein and the Ag surface is smaller than 3 Å, whereas an interaction is defined as persistent if the amino acid residue remains in contact with the metal for at least 60% of the total protein-metal surface interaction time.

The number of time each amino acid residue contacts the Ag surface and the number of persistent interactions realized are reported in **Figure 5.**

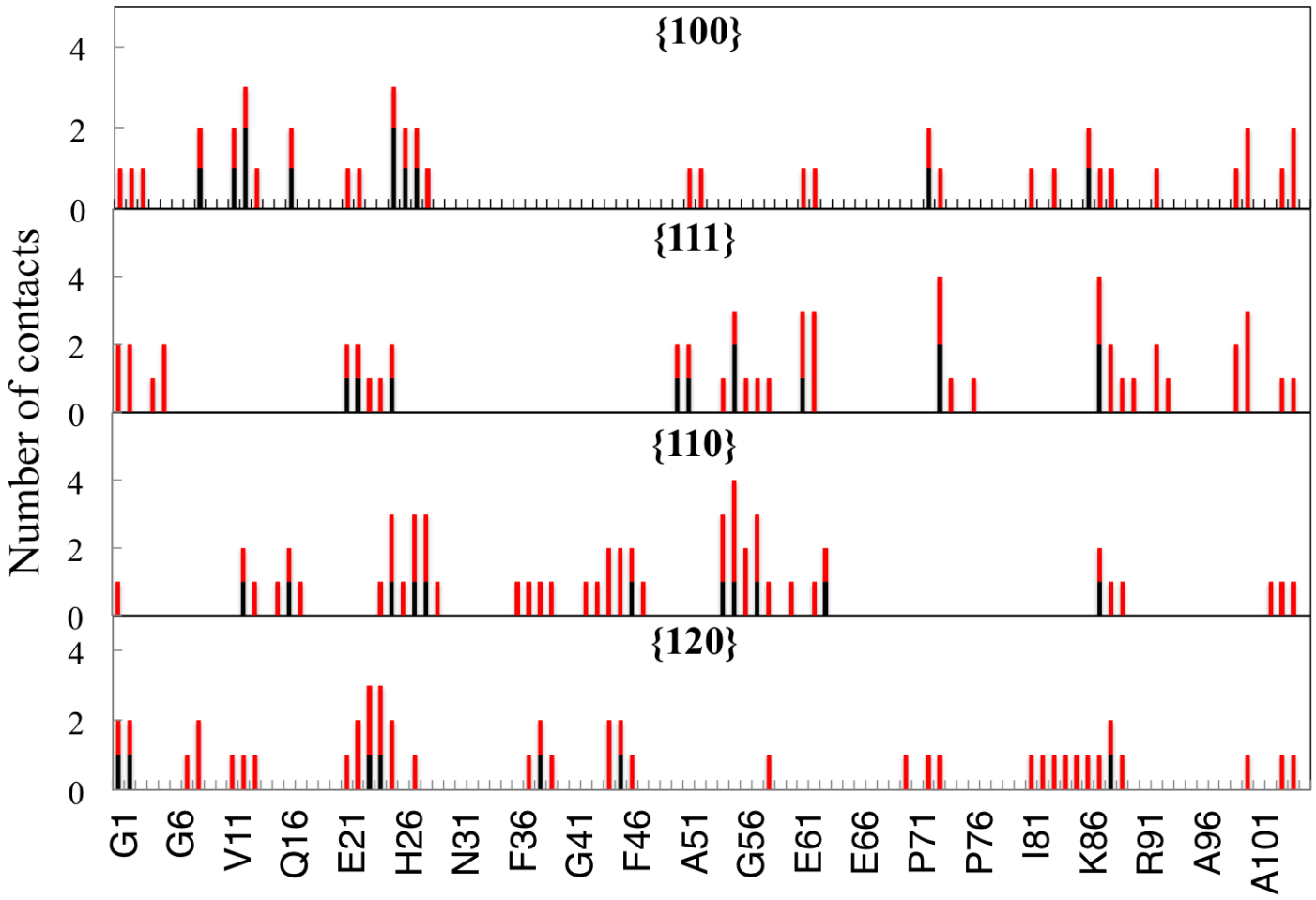


**Figure 5:** Number of contacts between the AA residues of CytC and different Ag facets occurring during the 100ns computational simulations. Red bars represent all the contacts realized during the simulations, while black bars represent amino acids that generate persistent interactions (over a 60% of the binding time) with the silver surface.

In the case of the Ag {100} a number of side-chains of charged amino acid residues crosses the structured water layer enabling the establishment of direct contacts with the surface (**Figure 5**). The most common persistent binding modes observed involve the clusters of residues K25-H26-K27 in Ω1 loop and K8-V11-Q12-Q16 in □-helix 1 (**Figure 6a,c**, and **Table 1**) whose interactions can be considered persistent with respect the total protein-metal surface interaction time. A third binding mode, observed for more than 60% of the total protein-metal surface interaction time, is realized by the side chains of K72 and K86 (**Figure 6b**).

Similarly, the binding of CytC to the Ag {111} facet involves the charged clusters of amino acids D50-A51-K55 in □-helix 2, E21-K22-K25 in Ω1 loop, and E61-K73-K87 in □-helix 3 (**Figure6 d,e,f**).

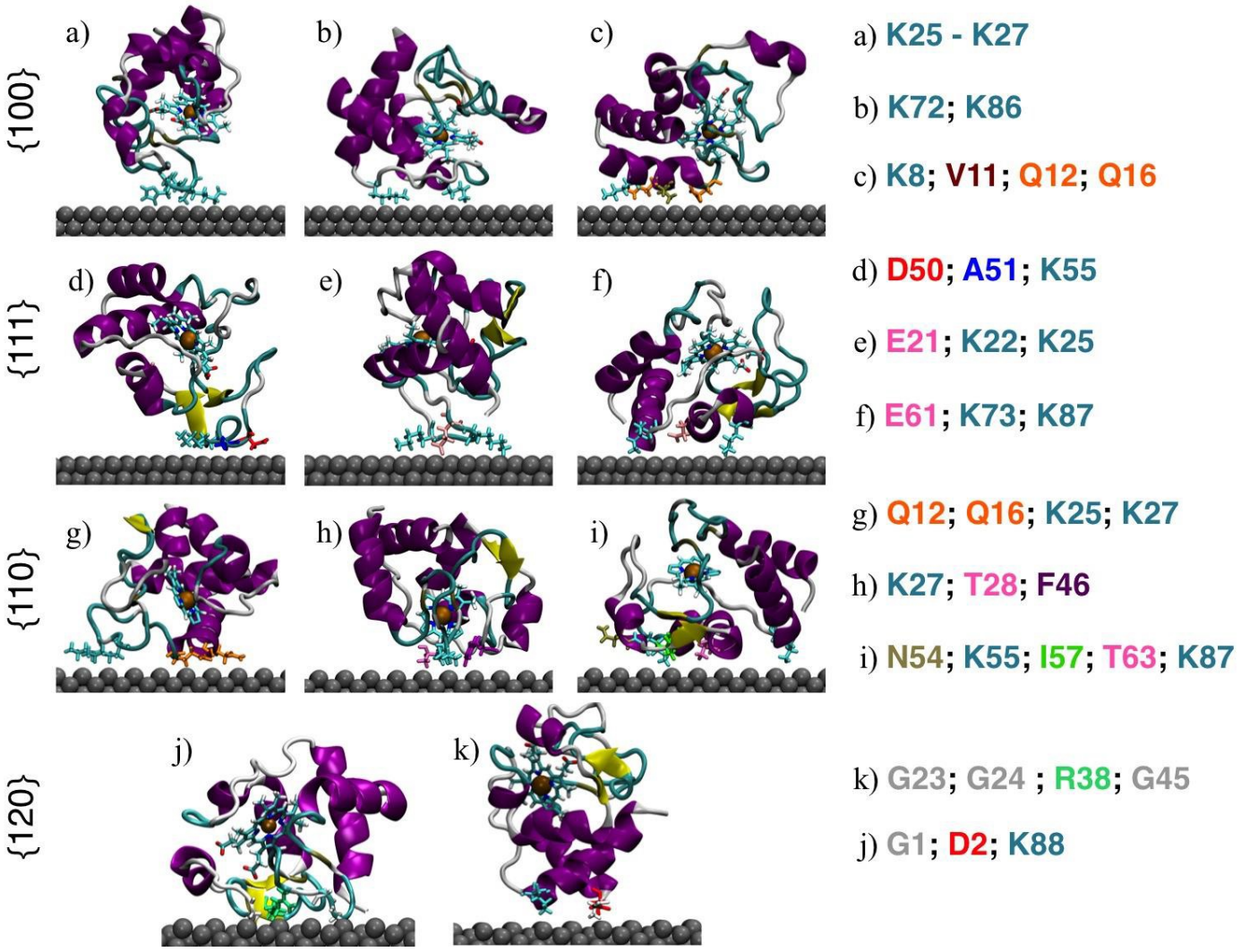


**Figure 6:** The main binding modes of CytC in its interaction with the Ag surfaces: a) to c) {100}, d) to f) the {111}, g) to i) {110} and j) to k) {120}. Amino acids that realize persistent interactions with the surfaces are shown for each configuration and they are coloured accordingly to their names, which are shown on the right. CytC is coloured accordingly to its secondary structures. Water molecules and ions are not shown for clarity.

The interaction with the Ag {110} surface is characterized by the highest number of amino acid residues, which contact the surface establishing persistent interactions (**Table 1**, and **Figure 5).** Also in this case, three main zones of interactions can be highlighted: the cluster formed by residues Q12-Q16-K25-K27 located at the end of □-helix 2 and in the Ω1 loop; K27-T28-F46 located in the Ω1 and Ω2 loop; N54-K55-I57-T63-K87 located in □-sheet 2, □-helix 3 and the Ω3 loop (**Figure 6g,h,i**).

Finally, only a few amino acids contribute to the final binding of CytC to the {120} facet; they are grouped in two clusters (G23-G24-R38-G45 belonging to the Ω1 loop omega and □-sheet 1, and G1-D2-K88 in □-helix 1 and □-helix 4) (**Figure 6j,k**) characterized by a marked a hydrophobic nature.

Although, the CytC binding to the Ag surfaces proved mainly unspecific, almost all binding sites contain at least one Lys amino acid (see **Figure 7** and **Table S.2**) providing persistent interactions, in agreement with previously published works[9,10,42] concerning the interaction of CytC on bare gold surface[9]. Briefly, Peng et al.[9] found that residues with long side chains, such as Lys residues, accounted for the strong VdW interactions to a bare {111} Au surface, whereas Cys14 and Cys17 residues, being embedded into the catalytic pocket and covalently bound to two vinyl groups of the heme, generate negligible interactions with it.

This similarity in the CytC behaviour of bovine heart (this work) and horse heart (Peng et al.[9] work) proteins with respect to the interaction with the metal surfaces is probably due to the presence of a high number of Lys residues on the surface of the two different species. In a subsequent study, Peng et al.[10] used molecular simulations to study the interactions of horse heart CytC with positively charged surfaces, modelled by $NH_2$ self-assembled monolayers (SAM). They found that CytC adsorbs with different orientations on the $NH_2$-SAM depending on the nature and concentration of small ions added. In particular, they found that phosphate ions promote the binding of CytC through several Lys residues (K13, K25, K27, K72, K79, K86, and K87). The same interacting behaviour was observed for CytC adsorbed on Au surfaces coated by COOH-SAM[42].

Visual inspection of the trajectories of the molecular simulation runs shows that the high number of contacts observed for Gly residues (**Figure 7**) are due to the fact that these residues come close to the surface once dragged by neighbour residues directly interacting with the metal, such as Lys and Pro (see **Table S.2**). This happens in particular i) for the {120} facet, where four over seven contacting residues are constituted by Gly residues; ii) for the {110} facet, where the same number of Gly and Lys residues (i.e. 5) establishes stable contacts. In agreement with previous observations[17], positive cooperativity is observed upon binding. In fact, the initial permeation of the water layer by Lysine residues facilitates the subsequent binding of spatially close residues. Conversely, no Gly residues in contact with the {100} surface were noted. Interestingly, other kinds of amino acids that preferentially interact with the Ag surfaces are Thr on the {110} surface, and Glu on the {111} (**Figure 7**).

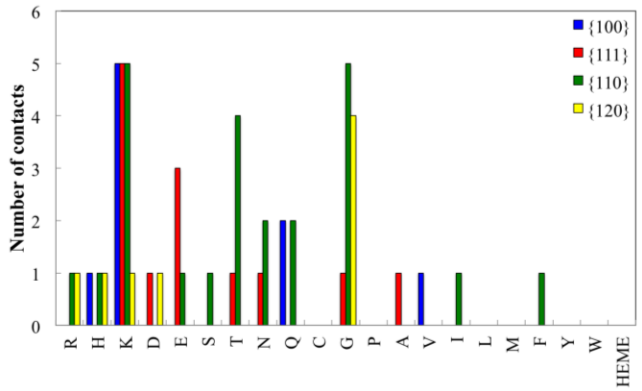


**Figure 7:** Total number of contacts of each amino acid residues. Only persistent interactions with the Ag surfaces are counted.

The heme group has never found to come into direct contact with the Ag surfaces. Moreover, no conformational changes involving the amino acids linked to the heme (C14, C17, H18, M80) have been observed during the simulation runs, in agreement with previous experimental observations.[13] In addition, as previously observed by computational simulations of CytC absorbed on bare gold surfaces[28] and on self-assembled monolayers[42,43] the overall secondary structure is well preserved during the adsorption. However, a careful comparison of the evolution of the secondary structure of the proteins over the dynamic runs (see **Figure S.3** in SI) reveals an higher mobility of the Ω1 loop (residues 20−30) and Ω2 loop (residues 40−49) of Cyt-c in interaction with the Ag {111} and Ag {100} surfaces with respect to the solvated unbound structure.

**Binding free energies**

The strength of the interaction between CytC and the Ag surfaces (binding free energy) has been calculated using the MM_PBSA algorithm[44] over the last 20 ns (2000 frames) of the simulations, i.e. in the period in which the proteins make persistent interactions and reach a stable bound configuration, as reported in the SI. For this reason, the results reported in **Figure 8a** show the maximum binding energies for each CytC –Ag surface complex, after the occurrence of a protein rearrangement to reach the optimal binding modalities[36,45]. In general, high-index facets show higher binding energies with respect to the {100} surface. However, the {111} and {110} surfaces show similar binding energies (~ -250 kcal/mol), whereas the binding of CytC to the {120} surface is weaker (~ -150 kcal/mol). It is worth noting that CytC adsorbed over the {111} surface shows the highest binding energy in spite of the low percentage of bound proteins (**Figure 8b**). This is an index of higher efficacy of binding of the CytC toward the {111} surface with respect to the other surfaces considered.

Similar findings were reported by Wright et al.[46] whose computational simulation study on peptide adsorption to gold {100} and {111} surfaces showed that the binding to the {111} is thermodynamically favoured in aqueous solution.

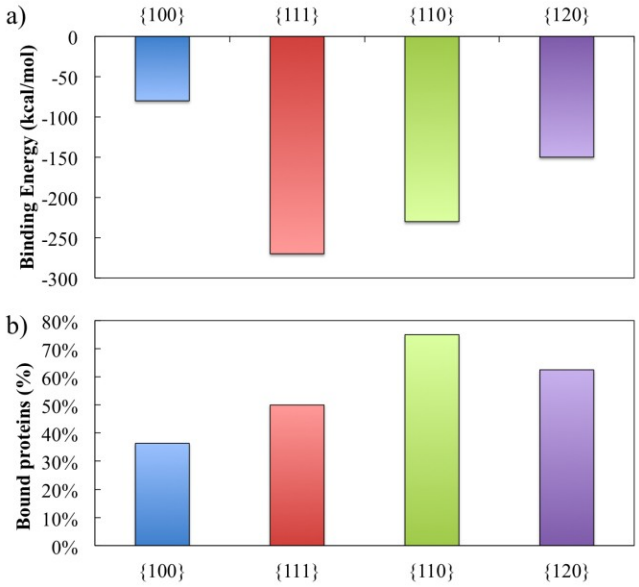


**Figure 8:** in panel (a) the maximum binding energy achieved by CytC in interaction with the {100}, {111}, {110} and {120} Ag surfaces. In panel (b), the percentage of proteins that make persistent interactions with each surface.

**PVP- capped Ag {100} surface**

In a recent experimental and computational study[13] some of us highlighted a preference of CytC to bind solvated Ag surfaces with respect to PVP capped surfaces. This behaviour was exploited to gather the protein at the round corner of silver nanocubes in order to obtain a site-selective SERS detection.

Since PVP is widely used as capping agent to stabilize nano-objects against agglomeration and regulate the growth rate of different crystal planes allowing the design of different anisotropic size/shaped nanostructures[47], a deeper analysis of the PVP-CytC interactions at atomic details may furnishes results of general interest in scientific approaches seeking to improve nanomedical applications.

**Figure 9** shows the results of the molecular simulation analysis of CytC-PVP interactions as detected by the time evolution of the minimum distance between eight CytC proteins and the PVP during the 100ns simulation.

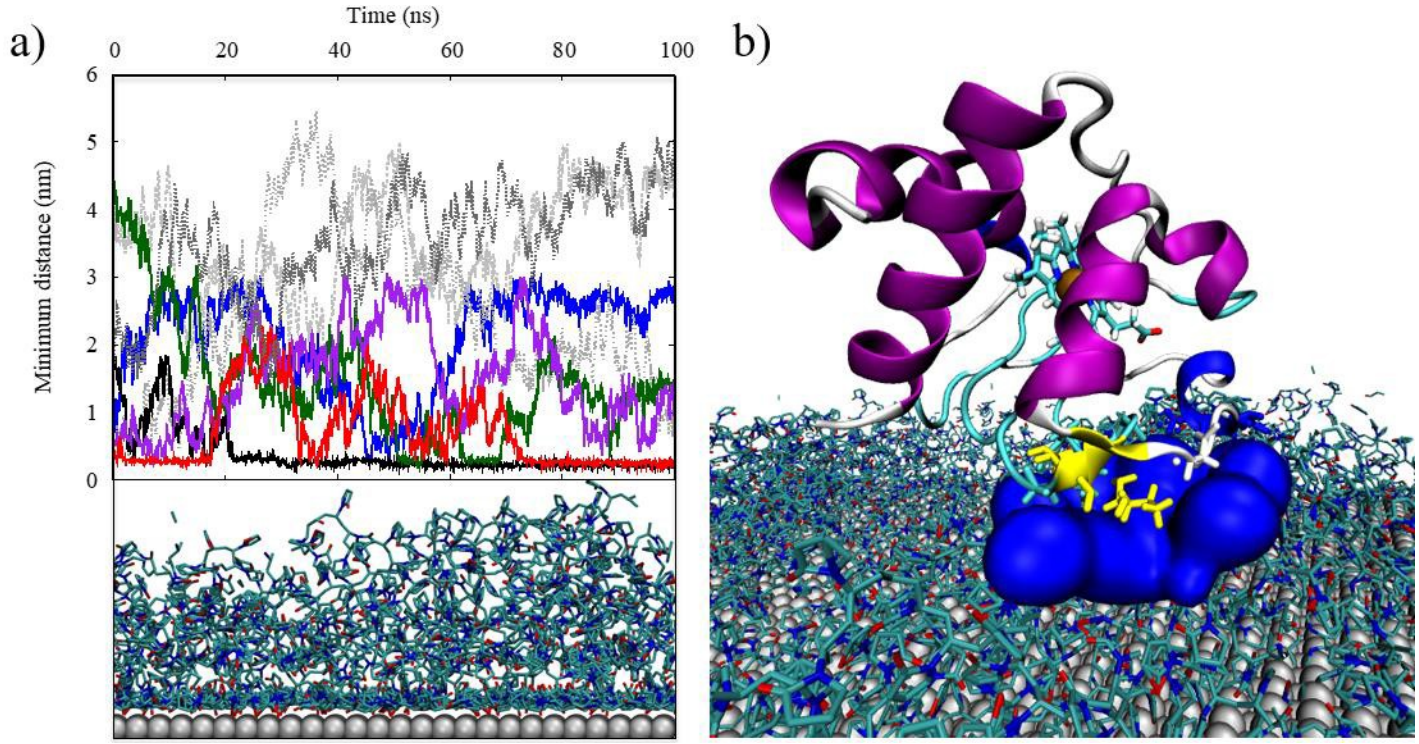


**Figure 9:** in panel a) the minimum distance between CytC and PVP during the simulation. The curves representing eight CytC proteins are shown in different colours. On the bottom the representation of the Ag surface covered by PVP. In panel b) a CytC interacting with PVP. The blue surface represents the PVP site of interaction with the protein.

The results show that the presence of the two polymer layers on the Ag surface hinders the direct contact of CytC and the metal. In fact, the crystal facet is completely shielded by the PVP polymer, in agreement with the experimental results on PVP coated silver nanoparticles reported by Ahlberg et al.[48]. In fact, only 1 out of 8 protein molecules considered in the molecular simulations (2 replicas with 4 CytC molecules each) is able to establish a permanent interaction with the outer layer of PVP. For five of the seven other proteins several adsorption/desorption events are observed during the length of the simulation runs (**Figure 9a**).

When a protein approaches the PVP outer layer, rearrangement of the polymer chains takes place in order to maximize the number of contacts with the protein (**Figure 9b and Figure S.4**). However, the PVP strands belonging to the first layer are firmly anchored to the metal surface by the oxygen and/or, the nitrogen in the 2-pyrrolidone ring[14,49] and cannot be displaced by the protein molecules. This behaviour was experimentally

observed also in case of PVP-coated Ag and Au nanoparticles once soaked in a biological medium with bovine serum albumin[50].

Interestingly, CytC shows a specific binding region to PVP ranging from Pro44 to Phe46, as showed in **Figure 10**, with a maximum binding energy of -45 kcal/mol, while other regions are never found to be in contact with the PVP layer. It is worth noting that this energetic result is of a mainly qualitative value. From a quantitative point of view, the value can be affected by a scarce statistical sampling since only one protein interacts persistently with the surface during the simulation run. However, overall, these finding are in agreement with previous finding by Ahlberg et al.[48] who showed that PVP coatings lower the binding affinities of nanoparticles for proteins of one order of magnitude with respect to citrate coatings, irrespective of the metallic core (silver or gold). Moreover, these results corroborate the scenario emerged by our previous experimental and computational study[13] on the interaction of CytC with PVP capped Ag nanocubes that claims for a preferential interaction of CytC to PVP-free edges and corners.

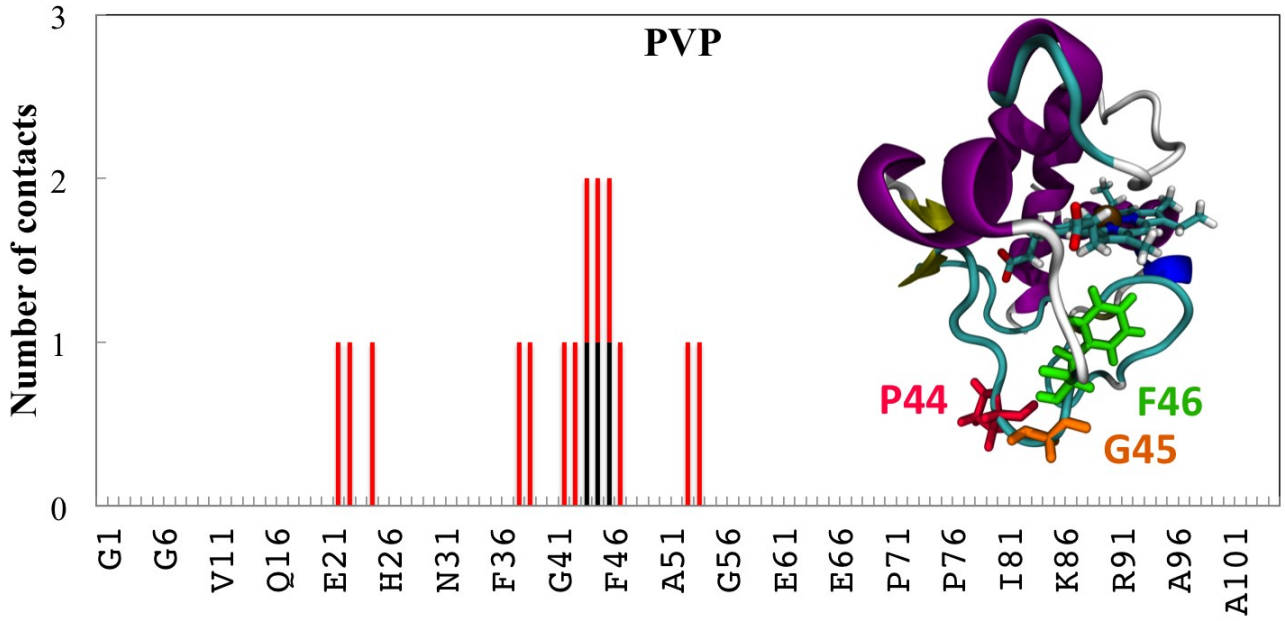


**Figure 10:** Number of contacts for each CytC amino acid with the PVP-coated Ag surface. Red data represent contacts computed from the beginning of the interaction, while black data represent amino acids that form persistent contacts (over a 60% of the binding time) with the PVP. The secondary structure representation of CytC with amino acids in contact with the PVP coloured in magenta (P44), orange (G45) and green (F46) is also shown.

## Conclusions

The results obtained by computational simulations of the interaction between CytC and wet silver surfaces, both bare and coated with PVP, furnish a general picture of the determinants for surface recognition and binding.

Differences in the approaching and early docking processes of CytC to the {100}, {111}, {110} and {120} Ag facets can be ascribed to an interplay of several determinants, related to the protein, the surface and the water. The ability of the protein to overwhelm the structure of the first layer of water over the Ag surfaces plays an important role in all the models studied. In general, amino acid residues with flexible side-chain, such as Lysine, are more prone to breaking through the bound water layer dragging neighbouring residues. Optimal interaction sites can then be realized in different way, giving rise to unspecific binding modes for all the metal surfaces. The binding sites involved spots spread over the whole CytC surface, but the heme group is never found to come into direct contact with the Ag surfaces. Moreover, the protein secondary structure undergoes minimal conformational changes. Therefore,

adsorption on the wet {100}, {111}, {110} and {120} Ag facets seems not to hamper electron transfer and produce loss of bioactivity of the CytC proteins.

The MM_PBSA maximum binding energy for each CytC –Ag surface complex, computed after the occurrence of protein rearrangement to reach the optimal binding modalities,[36,45] shows that high-index facets exhibit higher binding energies with respect to the {100} surface. The best efficacy of binding (i.e. binding energy *vs* percentage of bound proteins) is found toward the {111} surface.

As for the PVP coated surface, the double-layer polymer coating formed on the Ag surface mediates the interaction with the environment. Only a few persistent interactions are established between CytC and PVP during the simulation runs, the binding being realized in a specific way with the residues belonging to the □-sheet 1 stretch of amino acids and a lower maximum binding energy is achieved with respect to the wet pristine surface.

These results can be useful in driving the design of well-defined facets on nanocrystals, conferring them ideal features for optimal protein–surface interactions and specific diagnostic applications.

## Related content

### Supporting Information

Computational details of the model: dimension of the boxes used, Heme dipole angle. Data analysis: details on the computation of the Binding Energy (MM_PBSA). Protein adsorption: CytC adsorption on the {100} Ag surfaces; list of amino acids generating persistent contacts with the Ag surface. CytC secondary structure changes upon binding. PVP-rearrangement upon protein absorption.


## Acknowledgements

P.M. acknowledges the financial support from the Tuscany Region in the framework of PAR-FAS action line 1.1.2 SUPREMAL project. F.T and MCM acknowledges the financial support from MIUR Italian Ministero dell'Istruzione, dell'Università e della Ricerca (MIUR) Grant 2010C4R8M8_002.


## References


(1) Rosi, N. L.; Mirkin, C. A. Nanostructures in Biodiagnostics. *Chem. Rev.* **2005**, *105*, 1547−1562.

(2) Chen, G.; Roy, I.; Yang, C.; Prasad, P. N. Nanochemistry and Nanomedicine for Nanoparticle-Based Diagnostics and Therapy. *Chem. Rev.* **2016**, *116*, 2826−2885.

(3) Gray, J. J. The Interaction of Proteins with Solid Surfaces. *Curr. Opin. Struct. Biol.* **2004**, *14*,

110−115.

(4) Rabe, M.; Verdes, D.; Seeger, S. Understanding Protein Adsorption Phenomena at Solid Surfaces. *Adv. Colloid Interface Sci.* **2011**, *162*, 87−106.

(5) Mahmoudi, M.; Lynch, I.; Ejtehadi, M. R.; Monopoli, M. P.; Bombelli, F. B.; Laurent, S. Protein−Nanoparticle Interactions: Opportunities and Challenges. *Chem. Rev.* **2011**, *111*, 5610−5637.

(6) Ozboyaci, M.; Kokh, D. B.; Corni, S.; Wade, R. C. Modeling and Simulation of Protein−surface Interactions: Achievements and Challenges. *Q. Rev. Biophys.* **2016**, *49*, e4 (87 pages).

(7) Charchar, P.; Christofferson, A. J.; Todorova, N.; Yarovsky, I. Understanding and Designing the Gold−Bio Interface: Insights from Simulations. *Small* **2016**, *12*, 2395−2418.

(8) Heinz, H.; Ramezani-Dakhel, H. Simulations of Inorganic−bioorganic Interfaces to Discover New Materials: Insights, Comparisons to Experiment, Challenges, and Opportunities. *Chem Soc Rev* **2016**, *45*, 412−448.

(9) Peng, C.; Liu, J.; Zhou, J. Molecular Simulations of Cytochrome c Adsorption on a Bare Gold Surface: Insights for the Hindrance of Electron Transfer. *J. Phys. Chem. C* **2015**, *119*, 20773−20781.

(10) Peng, C.; Liu, J.; Xie, Y.; Zhou, J. Molecular Simulations of Cytochrome c Adsorption on Positively Charged Surfaces: The Influence of Anion Type and Concentration. *Phys. Chem. Chem. Phys.* **2016**, *18*, 9979−9989.

(11) Feng, J.; Slocik, J. M.; Sarikaya, M.; Naik, R. R.; Farmer, B. L.; Heinz, H. Influence of the Shape of Nanostructured Metal Surfaces on Adsorption of Single Peptide Molecules in Aqueous Solution. *Small Weinh. Bergstr. Ger.* **2012**, *8*, 1049−1059.

(12) Hughes, Z. E.; Walsh, T. R. Non-Covalent Adsorption of Amino Acid Analogues on Noble-Metal Nanoparticles: Influence of Edges and Vertices. *Phys. Chem. Chem. Phys.* **2016**, *18*, 17525−17533.

(13) Matteini, P.; Cottat, M.; Tavanti, F.; Panfilova, E.; Scuderi, M.; Nicotra, G.; Menziani, M. C.; Khlebtsov, N.; de Angelis, M.; Pini, R. Site-Selective Surface-Enhanced Raman Detection of Proteins. *ACS Nano* **2017**, *11*, 918−926.

(14) Xia, Y.; Xiong, Y.; Lim, B.; Skrabalak, S. E. Shape-Controlled Synthesis of Metal Nanocrystals: Simple Chemistry Meets Complex Physics? *Angew. Chem. Int. Ed.* **2009**, *48*, 60−103.

(15) Hildebrandt, P.; Stockburger, M. Surface-Enhanced Resonance Raman Spectroscopy of Cytochrome c at Room and Low Temperatures. *J. Phys. Chem.* **1986**, *90*, 6017−6024.

(16) Palafox-Hernandez, J. P.; Tang, Z.; Hughes, Z. E.; Li, Y.; Swihart, M. T.; Prasad, P. N.; Walsh, T. R.; Knecht, M. R. Comparative Study of Materials-Binding Peptide Interactions with Gold and Silver Surfaces and Nanostructures: A Thermodynamic Basis for Biological Selectivity of Inorganic Materials. *Chem. Mater.* **2014**, *26*, 4960−4969.

(17) Poblete, H.; Agarwal, A.; Thomas, S. S.; Bohne, C.; Ravichandran, R.; Phospase, J.; Comer, J.; Alarcon, E. I. New Insights into Peptide−Silver Nanoparticle Interaction: Deciphering the Role of Cysteine and Lysine in the Peptide Sequence. *Langmuir* **2016**, *32*, 265−273.

(18) Hughes, Z. E.; Wright, L. B.; Walsh, T. R. Biomolecular Adsorption at Aqueous Silver Interfaces: First-Principles Calculations, Polarizable Force-Field Simulations, and Comparisons with Gold. *Langmuir* **2013**, *29*, 13217−13229.

(19) Aliaga, A. E.; Ahumada, H.; Sepúlveda, K.; Gomez-Jeria, J. S.; Garrido, C.; Weiss-López, B. E.; Campos-Vallette, M. M. SERS, Molecular Dynamics and Molecular Orbital Studies of the MRKDV Peptide on Silver and Membrane Surfaces. *J. Phys. Chem. C* **2011**, *115*, 3982−3989.

(20) Mirkin, N.; Jaconcic, J.; Stojanoff, V.; Moreno, A. High Resolution X-Ray Crystallographic Structure of Bovine Heart Cytochrome c and Its Application to the Design of an Electron Transfer Biosensor. *Proteins* **2008**, *70*, 83−92.

(21) Berman, H. M.; Westbrook, J.; Feng, Z.; Gilliland, G.; Bhat, T. N.; Weissig, H.; Shindyalov, I. N.; Bourne, P. E. The Protein Data Bank. *Nucleic Acids Res.* **2000**, *28*, 235−242.

(22) MacKerell, A. D.; Bashford, D.; Bellott, M.; Dunbrack, R. L.; Evanseck, J. D.; Field, M. J.; Fischer, S.; Gao, J.; Guo, H.; Ha, S.; *et al.* All-Atom Empirical Potential for Molecular Modeling and Dynamics Studies of Proteins. *J. Phys. Chem. B* **1998**, *102*, 3586−3616.

(23) Autenrieth, F.; Tajkhorshid, E.; Baudry, J.; Luthey-Schulten, Z. Classical Force Field Parameters for the Heme Prosthetic Group of Cytochrome c. *J. Comput. Chem.* **2004**, *25*, 1613−1622.

(24) Heinz, H.; Vaia, R. A.; Farmer, B. L.; Naik, R. R. Accurate Simulation of Surfaces and Interfaces of Face-Centered Cubic Metals Using 12-6 and 9-6 Lennard-Jones Potentials. *J. Phys. Chem. C* **2008**, *112*, 17281−17290.

(25) Penna, M. J.; Mijajlovic, M.; Biggs, M. J. Molecular-Level Understanding of Protein Adsorption at the Interface between Water and a Strongly Interacting Uncharged Solid Surface. *J. Am. Chem. Soc.* **2014**, *136*, 5323−5331.

(26) Iori, F.; Di Felice, R.; Molinari, E.; Corni, S. GolP: An Atomistic Force-Field to Describe the Interaction of Proteins with Au(111) Surfaces in Water. *J. Comput. Chem.* **2009**, *30*, 1465−1476.

(27) Iori, F.; Corni, S. Including Image Charge Effects in the Molecular Dynamics Simulations of Molecules on Metal Surfaces. *J. Comput. Chem.* **2008**, *29*, 1656−1666.

(28) Kyrychenko, A.; Korsun, O. M.; Gubin, I. I.; Kovalenko, S. M.; Kalugin, O. N. Atomistic Simulations of Coating of Silver Nanoparticles with Poly(vinylpyrrolidone) Oligomers: Effect of Oligomer Chain Length. *J. Phys. Chem. C* **2015**, *119*, 7888−7899.

(29) Darden, T.; York, D.; Pedersen, L. Particle Mesh Ewald: An N·log(N) Method for Ewald Sums in Large Systems. *J. Chem. Phys.* **1993**, *98*, 10089−10092.

(30) Essmann, U.; Perera, L.; Berkowitz, M. L.; Darden, T.; Lee, H.; Pedersen, L. G. A Smooth Particle Mesh Ewald Method. *J. Chem. Phys.* **1995**, *103*, 8577−8593.

(31) Hughes, Z. E.; Walsh, T. R. Structure of the Electrical Double Layer at Aqueous Gold and Silver Interfaces for Saline Solutions. *J. Colloid Interface Sci.* **2014**, *436*, 99−110.

(32) Hess, B. P-LINCS: A Parallel Linear Constraint Solver for Molecular Simulation. *J. Chem. Theory Comput.* **2008**, *4*, 116−122.

(33) Abraham M. J.; van der Spoel D.; Lindahl E.; Hess B.; and the GROMACS development team. GROMACS: High Performance Molecular Simulations through Multi-Level Parallelism from Laptops to Supercomputers. *GROMACS User Man. Version 504*.

(34) Humphrey, W.; Dalke, A.; Schulten, K. VMD: Visual Molecular Dynamics. *J. Mol. Graph.* **1996**, *14*, 33−38, 27−28.

(35) Limmer, D. T.; Willard, A. P.; Madden, P.; Chandler, D. Hydration of Metal Surfaces Can Be Dynamically Heterogeneous and Hydrophobic. *Proc. Natl. Acad. Sci.* **2013**, *110*, 4200−4205.

(36) Wang, A.; Vangala, K.; Vo, T.; Zhang, D.; Fitzkee, N. C. A Three-Step Model for Protein−Gold Nanoparticle Adsorption. *J. Phys. Chem. C* **2014**, *118*, 8134−8142.

(37) Tavanti, F.; Pedone, A.; Menziani, M. C. A Closer Look into the Ubiquitin Corona on Gold Nanoparticles by Computational Studies. *New J. Chem.* **2015**, *39*, 2474−2482.

(38) Tavanti, F.; Pedone, A.; Menziani, M. C. Competitive Binding of Proteins to Gold Nanoparticles Disclosed by Molecular Dynamics Simulations. *J. Phys. Chem. C* **2015**, *119*, 22172−22180.

(39) Ozboyaci, M.; Kokh, D. B.; Wade, R. C. Three Steps to Gold: Mechanism of Protein Adsorption Revealed by Brownian and Molecular Dynamics Simulations. *Phys. Chem. Chem. Phys.* **2016**, *18*, 10191−10200.

(40) Yu, J.; Becker, M. L.; Carri, G. A. The Influence of Amino Acid Sequence and Functionality on the Binding Process of Peptides onto Gold Surfaces. *Langmuir* **2012**, *28*, 1408−1417.

(41) Hughes, Z. E.; Kochandra, R.; Walsh, T. R. Facet-Specific Adsorption of Tripeptides at Aqueous Au Interfaces: Open Questions in Reconciling Experiment and Simulation. *Langmuir*

**2017**, *33*, 3742−3754.

(42) Zhou, J.; Zheng, J.; Jiang, S. Molecular Simulation Studies of the Orientation and Conformation of Cytochrome c Adsorbed on Self-Assembled Monolayers. *J. Phys. Chem. B* **2004**, *108*, 17418−17424.

(43) Xu, J.; Bowden, E. F. Determination of the Orientation of Adsorbed Cytochrome c on Carboxyalkanethiol Self-Assembled Monolayers by In Situ Differential Modification. *J. Am. Chem. Soc.* **2006**, *128*, 6813−6822.

(44) Kumari, R.; Kumar, R.; Lynn, A. g_mmpbsa—A GROMACS Tool for High-Throughput MM-PBSA Calculations. *J. Chem. Inf. Model.* **2014**, *54*, 1951−1962.

(45) Tavanti, F.; Pedone, A.; Menziani, M. C. A Closer Look into the Ubiquitin Corona on Gold Nanoparticles by Computational Studies. *New J. Chem.* **2015**, *39*, 2474−2482.

(46) Wright, L. B.; Palafox-Hernandez, J. P.; Rodger, P. M.; Corni, S.; Walsh, T. R. Facet Selectivity in Gold Binding Peptides: Exploiting Interfacial Water Structure. *Chem Sci* **2015**, *6*, 5204−5214.

(47) Xia, X.; Zeng, J.; Zhang, Q.; Moran, C. H.; Xia, Y. Recent Developments in Shape-Controlled Synthesis of Silver Nanocrystals. *J. Phys. Chem. C* **2012**, *116*, 21647−21656.

(48) Ahlberg, S.; Antonopulos, A.; Diendorf, J.; Dringen, R.; Epple, M.; Flöck, R.; Goedecke, W.; Graf, C.; Haberl, N.; Helmlinger, J.; *et al.* PVP-Coated, Negatively Charged Silver Nanoparticles: A Multi-Center Study of Their Physicochemical Characteristics, Cell Culture and in Vivo Experiments. *Beilstein J. Nanotechnol.* **2014**, *5*, 1944−1965.

(49) Al-Saidi, W. A.; Feng, H.; Fichthorn, K. A. Adsorption of Polyvinylpyrrolidone on Ag Surfaces: Insight into a Structure-Directing Agent. *Nano Lett.* **2012**, *12*, 997−1001.

(50) Treuel, L.; Malissek, M.; Grass, S.; Diendorf, J.; Mahl, D.; Meyer-Zaika, W.; Epple, M. Quantifying the Influence of Polymer Coatings on the Serum Albumin Corona Formation around Silver and Gold Nanoparticles. *J. Nanoparticle Res.* **2012**, *14*, 1102.

## Table of Contents Graphic